AJ ACADEMIC JOURNALS
expand your knowledge

International Journal of Physical Sciences

Full Length Research Paper

Adsorption and Thermodynamic studies of the corrosion inhibition effect of *Rosmarinus Officinalis* L. leaves on aluminium alloy in 0.25 M HCl and effect of an external magnetic field

Paul A. Andoor*, Kelechukwu B. Okeoma and Uchenna S. Mbamara

Department of Physics, School of Physical Sciences, Federal University of Technology, PMB 1526 Owerri, Imo State, Nigeria.

The corrosion inhibition of Aluminium alloy AA8011 in 0.25 M hydrochloric acid solution by *Rosmarinus officinalis* L. (rosemary) leaves extract was studied using the gravimetric technique at 303, 313, 323 and 333K, and in the presence of an external magnetic field. The study reveals that the methanolic extract of rosemary leaves inhibits corrosion of Al in 0.25 M HCl. The inhibition efficiency was found to increase with increase in concentration of the extract, but decreased with increase in temperature. Thermodynamic activation parameters like the activation energy (E_a), ranged from 15.29 to 35.06 kJ/mol, thereby suggesting the mix mechanism of physichemisorption; calculated values of the standard adsorption enthalpies (ΔH_{ads}^o) were positive indicating an endothermic process, while negative values of entropies (ΔS_{ads}^o) implied an associative interaction between the inhibitor molecules and the Al surface. The corrosion data was found to be a good fit for the Langmuir ($R^2 > 0.98$) and Villamil ($R^2 > 0.99$) isotherm models. Values of the adsorption free energy (ΔG_{ads}^o) obtained were negative, thereby describing a spontaneous adsorption process. The effect of an external magnetic field was found to have a mixed behaviour in the presence of the *R. offinalis* L. extract at room temperature. Nonetheless, the corrosion rate was generally found to decrease with increase in strength of the magnetic field.

Key words: Acid corrosion, rosemary, aluminium, langmuir model, magnetic field.

INTRODUCTION

Aluminium makes up about 8.3% of the earth's crust and is the most widely used non-ferrous alloy Millberg (2018). Aluminium and its alloys are extensively used in the area of transportation, construction of bridges and buildings, fabrication of electrical machinery/equipment, and is the choice material for packaging food and beverages

*Corresponding author. E-mail: paulandoor@gmail.com.

(Maghraby, 2009; Chaubey et al., 2018; Popoola et al., 2012). Its wide range of applications is due to its low price, high strength-to-weight ratio, high electrical and thermal conductivities (Sukiman et al., 2012). In addition, aluminium is generally non-toxic, paramagnetic, and possesses high resistance to atmospheric or environmental corrosion Davis (1993). The corrosion resistance of aluminium is due to its ability to readily passivate, to form a tough, inert thin oxide film on its surface almost immediately when exposed to the atmosphere (Noor, 2009; Hansson 2011; Sangeetha et al, 2013) thereby reducing its susceptibility to corrosion (Abdallah et al. (2013).

However, this protective film is known to deteriorate in the presence of very aggressive acidic media containing Cl⁻ ions (El-Awady et al., 1993; Jegdić et al., 2016; Lowson, 1978) like seawater, as well as solutions of hydrochloric acid (HCl) used for pickling, chemical, and electrochemical etching of aluminium (Khan et al., 2015; Philip and Schweitzer, 2003). Several factors like temperature, and the presence of a magnetic field can greatly affect the corrosion rate of Al in HCl media (Davis, 1993; Philip and Schweitzer, 2003)

The corrosion of aluminium and its alloy is destructive and poses an extremely costly problem (Gilbert, 1978). There are several methods of corrosion control, however, focus has shifted to the use of green inhibitors, that is, plant extracts (either from the leaves, seeds, fruits, or even roots) as a low-cost, eco-friendly alternative to synthesized organic inhibitors (Velázquez-González et al, (2014); Kesavan et al. (2012) Manimegalai and Manjula, 2015). Green inhibitors contain neither toxic compounds nor heavy metals. When introduced in very small concentrations, certain heteroatoms like O, P, S, and N (Khan et al., 2015) present in organic compounds like tannins, amino acids, dyes and alkaloids found in the plants extracts help adsorb these compounds onto the surface of the metal by displacing water molecules, thereby forming a protective film (Patni et al., 2013) which inhibits further corrosion.

The rosemary plant (*Rosmarinus officinalis* L.) is the green inhibitor of choice studied in this paper. It is an aromatic plant of Mediterranean origin (Velázquez-González et al, (2014) and contains rosmarinic acid as its active ingredient, in addition to antioxidants like carnosic acid and carnosol (Rani and Basu, 2012; Fouda et al., 2015; Francis et al., 2019; Barbut et al., 1985; Nakatani, 2000), therefore making it one of the most widely used and commercialized green inhibitors (Fouda et al., 2015; Deyab, 2016; Catic et al., 2016). The structure of its active constituents is as shown in Figure 1 (Velázquez-González et al., 2014).

The presence of the heteroatom (O) in their aromatic rings suggests that *R. officinalis* L. can be a possible corrosion inhibitor for Al. Materials are classified as ferromagnetic, anti-ferromagnetic paramagnetic (like in the case of Al) or diamagnetic based on their behavior in the presence of an induced magnetic field (Myers, 1997). It is therefore expected that the presence of external magnetic field can have an influence in a chemical reaction involving such materials (Catic et al., 2016). Hence, this study seeks to investigate the corrosion inhibitive potential of *R. officinalis* L. on aluminium alloy in 0.25 M HCl at various temperatures, and the effect of the presence of an external magnetic field at room temperature (303K).

EXPERIMENTAL

Materials

Aluminium specimen

The commercial aluminium alloy AA8011 sheet used in this study was analyzed using optical emission spectrometry (OES), and had the following chemical composition in percent weight: Al-97.856%, Fe-0.901%, Si-0.375%, Mg-0.374%, Zn-0.209%, Cu-0.157%, Mn-0.111%, Ti-0.005%, Ni-0.004%, and other trace elements. The Al sheet was cut into coupons of dimensions of ~30 mm × ~30 mm × ~1 mm and each housing a ⌀2 mm bore.

Rosemary leaves

Freshly harvested rosemary herb separated from it stem and room dried.

Chemicals

All chemicals used were of analytical grade:

(a) Hydrochloric acid (HCl) solution by JHD® with a purity of (35.5-37.5% wt) used as the corroding media,
(b) Nitric acid (HNO₃) (65% purity) solution used as quenching media,
(c) Methanol (purity 99.5%) by LOBAL Chemie used for the cold extraction of the rosemary herb,
(d) Acetone Extra Pure (purity 99.0%) by LOBAL Chemie was used for rinsing.

Method

The gravimetric technique

The gravimetric method is simple and reliable, and forms the baseline method for many corrosion inhibition assessment programs (Beda et al, 2017). To study the corrosion behavior of Al in an aggressive media like HCl, attempt was made to quantify the degree of dissolution of the Al coupons in a solution of the corrodant for a given amount of time by computing the mass loss. This was achieved by first finding the initial weight of the Al specimens. Prior to this, the Al specimens were hand-polished using SiC emery paper, washed with detergent, degreased using acetone, then dried at room temperature. The initial weight w_0 was obtained for each coupon using an electronic balance having an accuracy of ±0.001 g. A Vernier caliper was used to measure the
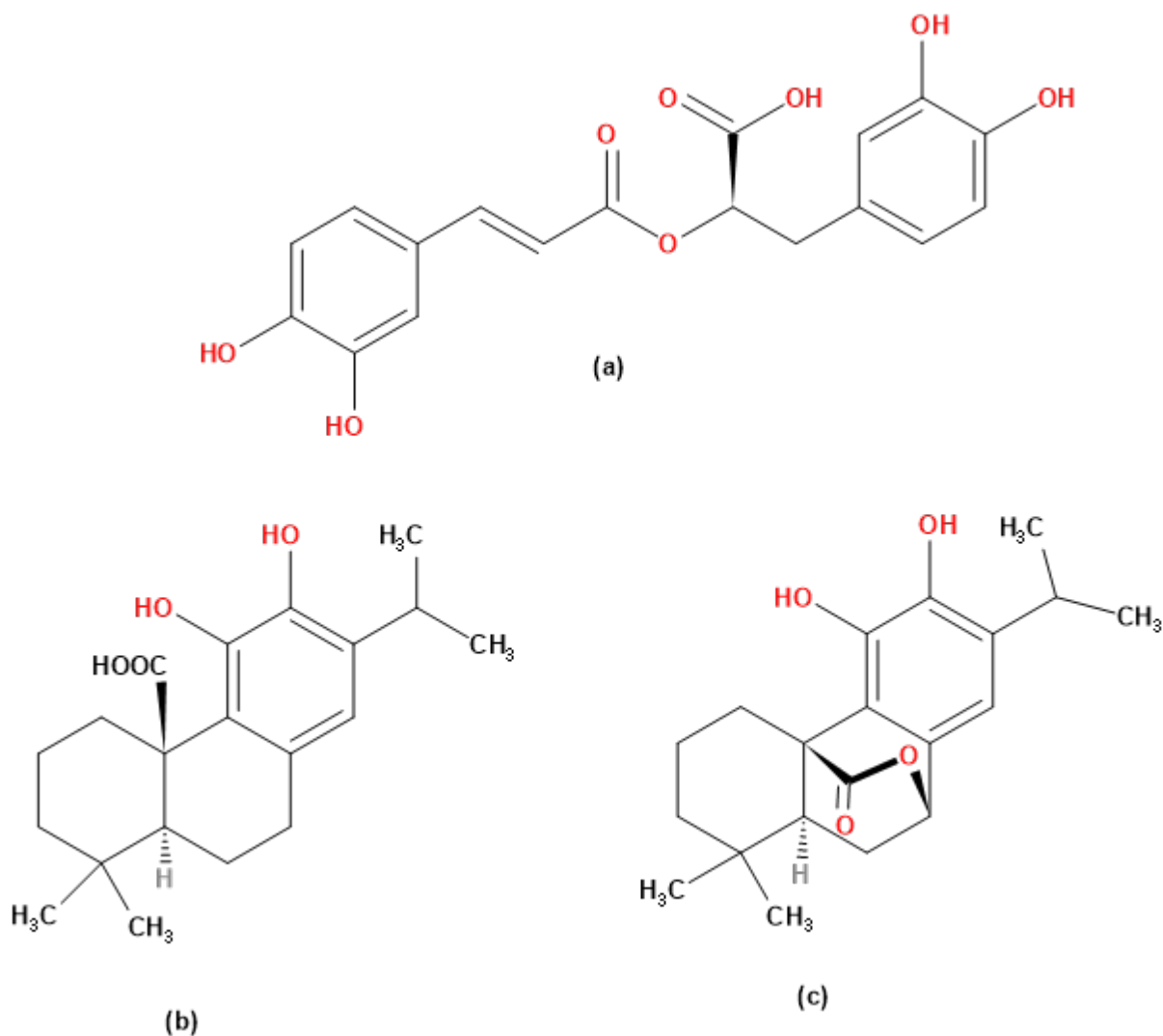
Figure 1. Chemical structure for the main components in *Rosmarinus officinalis* L. (a) Rosmarinic acid (b) Carnosic acid and (c) Carnosol.

full dimension l, b, and t of each coupon. The total exposed surface area, A_c for each coupon was computed using the formula:

$$A_c = 2lb + 2lt + 2bt + 2\pi rt - 2\pi r^2 \qquad (1)$$

where r is the radius of the hole on each coupon which was ~1 mm.

The total volume V, for each coupon was computed using:

$$V = lbt - \pi r^2 t \qquad (2)$$

The density (ρ) of each coupon was obtained from the ratio of the initial weight, w_0 of the coupons to the volume V according to the following equation:

$$\rho = \frac{w_0}{V} \qquad (3)$$

The average experimental density of the Al alloy coupons was obtained to be ~2.724 g/cm³ which is close to the theoretical value of 2.71 g/cm³.

The 0.25 M of HCl solution was prepared using the dilution equation. The resulting solution recorded a pH of 0.4 on a pocket-sized pH tester, while the preparation of the rosemary leaves extract was carried via the cold extraction method using methanol. For the preparation of the herb, 300 ml of methanol was introduced into the container containing 25.0 g of ground rosemary herbs. The resulting mixture was tightly sealed and then left for 24 h, after which it was sieved using a clean white handkerchief. The resulting filtrate served as the stock solution from which concentrations of

Figure 2. Schematics of the set-up for the use of magnetic field.

50, 150, 250, 500 and 1000 mg/L were obtained.

The mass loss experiment was carried out by totally immersing the Al coupons into glass vessels containing about 250 ml of 0.25 M HCl solution both in the absence (blank experiment) and presence of the *R. officinalis* L. extract (inhibited experiment). A thermometer was used to regulate the bath temperature for both the blank and inhibited experiments at 303K, 313K, 323K and 333K. After an exposure time of 3 h, the coupons were undipped from their solutions, quenched in 2.0 M HNO$_3$ solution, rinsed in ethanol and degreased in acetone, and then left to air-dry. The final weight, w_f obtained from the analytical weighing balance was used to compute the weight loss Δw in grams (g):

$$\Delta w = w_f - w_0 \tag{4}$$

In corrosion science, there is a fundamental quantity, the corrosion rate quantifies this degree of dissolution (Abdallah et al, 2013). The gravimetric corrosion rate, $C.R.$ in millimeter per year (mm/year) was computed using:

$$C.R. = \frac{k\Delta w}{\rho At} \tag{5}$$

where $k = 8.75 \times 10^3$, ρ is the average density of all the coupons in g/mm^3, A is the area of the Al coupon in mm^2, and t is the exposure time in hours.

The inhibitor efficiency of the *R. officinalis* L. extract was computed using the equation:

$$I.E.(\%) = \frac{CR_0 - CR_{inh}}{CR_0} \times 100 \tag{6}$$

where CR_0 and CR_{inh} are the corrosion rates in the absence and presence of inhibitor, respectively.

To study the effect of an external magnetic field on the inhibition behaviour of *R. officinalis* L. extract on the Al alloy, a magnetic field source with a variable voltage of up to 26.0 volts was used. The electromagnets were placed on either side of the glass vessel housing the Al coupons and HCl solution. The coupons were positioned transversally to the direction of the magnetic field as shown in Figure 2.

This experiment was performed at ambient temperature with input voltages of (Khan et al., 2015); Manimegalai and Manjula, 2015; and Barbut et al, 1985) volts in the presence of the inhibitor for 3 h, with the strength of a magnetic field, B directly proportional to the applied voltage, V according to the relation:

$$B \alpha \frac{V}{R_l l} \tag{7}$$

where R_l is the resistance per unit length of the solenoid wire, and l is the length of a turn.

## RESULTS AND DISCUSSION

Gravimetric measurements

The variation in the corrosion rate of Al at room temperature for an exposure time of up to 10 days is as shown in Figure 3. The figure shows a steady decrease in corrosion rate of Al in 0.25 M HCl and tends to take on a more linear relationship with increase in exposure time. This is in agreement with the results obtained by (Nwosu et al., 2018).

Effect of temperature

Temperature has a significant influence in the corrosion rate of metals (Ibisi and Uwakwue, 2015). This was verified for Al in 0.25 M HCl as shown in Figure 4 which shows a plot of values for the weight loss (g) obtained via Equation 4 for the blank experiment against an exposure time of 3 h.

Figure 4 shows that the values of weight loss (g) increase with increase in temperature. The corrosion rates and efficiencies at all temperatures for both the blank and inhibited experiments in 0.25 M HCl solution were calculated and listed in Table 1.

On inspection of Table 1 it is observed that the rate of degradation of Al in 0.25 M HCl increases with increase in temperature, but decreases with increase in concentration of the rosemary extract. The highest efficiency (68.68%) was obtained at 1000 mg/L concentration of inhibitor at 303K. This suggests that ambient temperature is the optimal operating temperature for the *R. officinalis* L. extract in 0.25 M HCl solution, and a decrease in the inhibitor efficiency with increase in temperature may be due to the increased rate of desorption of molecules of the *R. officinalis* L. extract from the adsorbent surface. Figure 5 shows a plot of the corrosion rate at 0.25 M HCl solution against temperature.
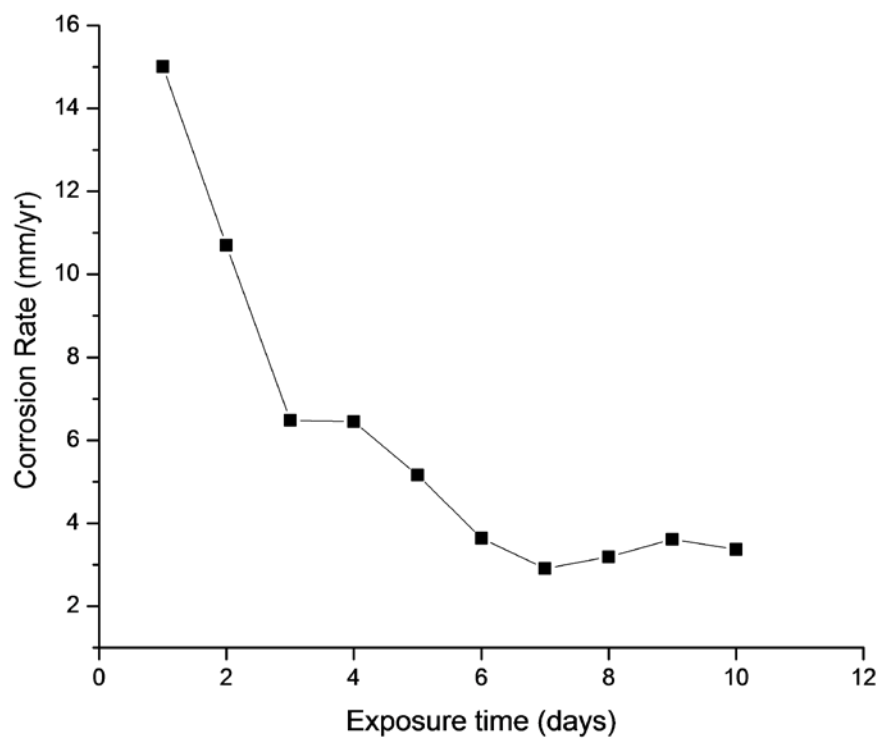
Figure 3. Corrosion rate variation with time for 0.25 M at room temperature.
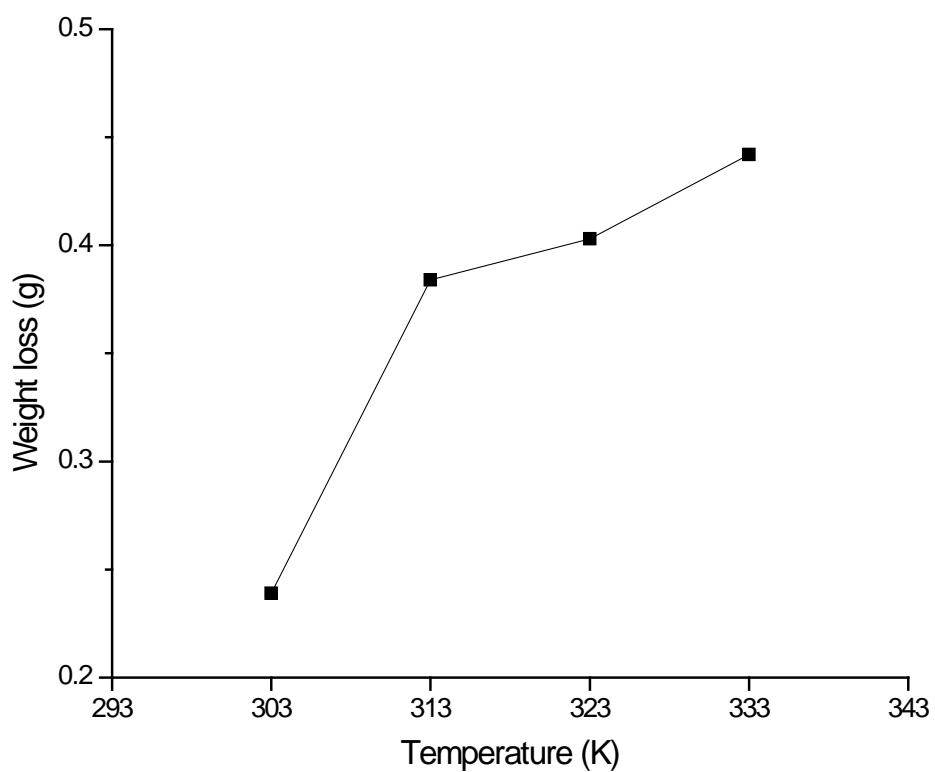
Figure 4. Weight loss (g) curve for Al alloy in 0.25 M HCl at different temperatures for the blank experiment.

Table 1. Calculated values for the corrosion rate and inhibitor efficiency at various temperatures for Al alloy corrosion in 0.25 M HCl solution.

Concentration (mg/L)	Corrosion rate (mm/year)				Inhibitor efficiency (%)			
	303K	313K	323K	333K	303K	313K	323K	333K
Blank	135.33	204.77	223.00	226.41	–	–	–	–
50	95.09	105.71	146.62	156.51	29.73	48.37	34.25	30.88
150	60.41	91.93	110.65	149.97	55.36	55.10	50.38	33.76
250	83.77	91.51	116.67	138.72	38.10	55.31	47.68	38.73
500	51.40	79.68	113.69	141.47	62.02	61.09	49.02	37.52
1000	42.38	67.42	110.71	144.22	68.68	67.07	50.35	36.30
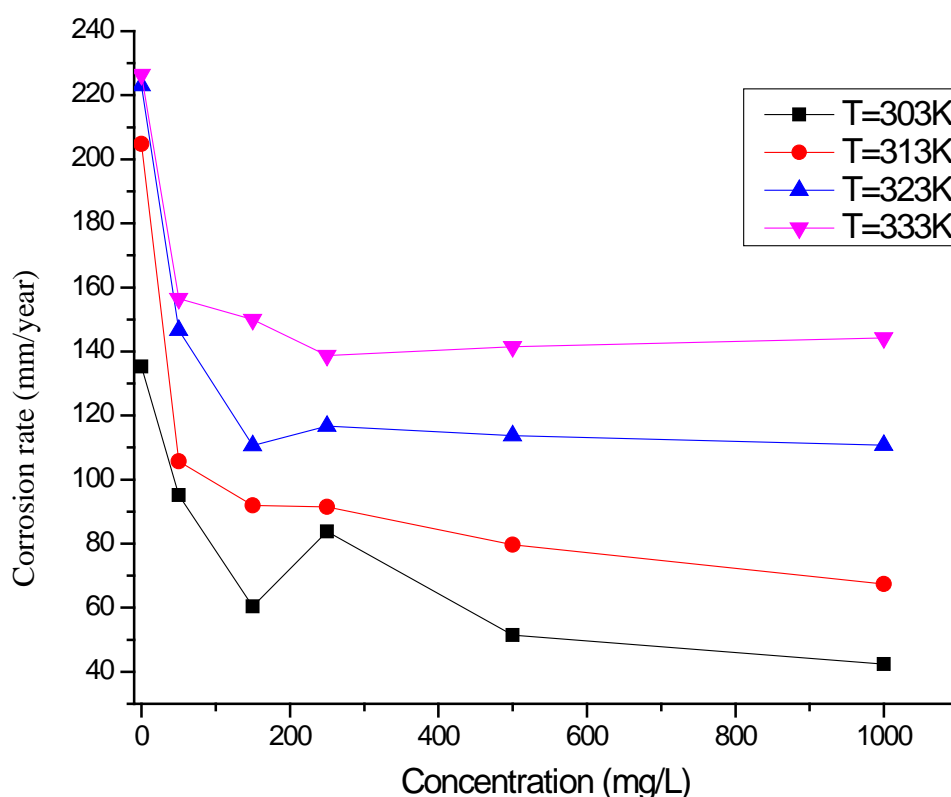
Figure 5. Corrosion rate of Al in 0.25 M HCl against concentration of Rosmarinus officinalis L. for all temperatures.

On inspection of the Figure 5, a general decrease in corrosion rate was observed with increase in concentration of the *R. officinalis* L. leaves extract. However, the effect of temperature is such that it tends to increase the corrosion rate with the highest recorded corrosion rates being observed at T=333K.

For the thermodynamic studies, the activation energy (E_a) is an important parameter in adsorption thermodynamic studies as it determines the temperature-dependence of the corrosion rate. It gives the minimum amount of energy required for the onset of an adsorbate-adsorbent interaction (Saha and Chowdhury, 2011). Since the Arrhenius equation relates a rate constant to the activation energy; hence,

$$CR = A \exp\left(-\frac{E_a}{RT}\right) \qquad (8)$$

where CR is the corrosion rate, A is the Arrhenius or
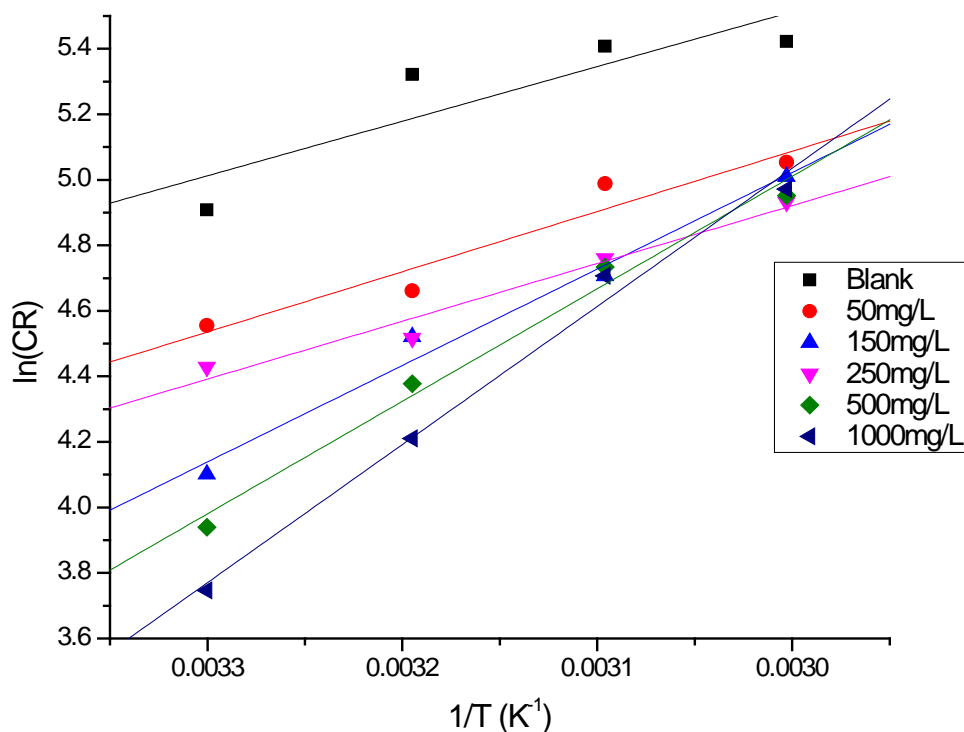
Figure 6. Arrhenius plot for Al alloy corrosion in 0.25 M HCl solution for blank and different concentrations of *Rosmarinus officinalis* L.

Table 2. Activation parameters of Al alloy in 0.25 M HCl for blank and different concentrations of *Rosmarinus officinalis* L.

Concentration (mg/L)	E_a (kJ/mol)	ΔH° (kJ/mol)	ΔS° (kJ/mol-K)
Blank	13.87	11.23	-1.64
50	15.29	12.65	-1.68
150	24.48	21.85	-3.11
250	14.67	12.04	-1.51
500	28.56	25.92	-3.74
1000	35.06	32.42	-4.78

pre-exponential factor, T is the temperature in kelvin (K), R is the gas constant (8.314 Jmol^{-1}K^{-1}). Linearizing Equation 8 by taking the logarithm of both sides gives:

$$\ln(CR) = \ln A - \frac{E_a}{RT} \qquad (9)$$

Values of $\ln(CR)$ plotted against $\frac{1}{T}$ to obtain straight lines whose gradients are $\frac{-E_a}{R}$ is as shown in Figure 6.

Straight lines were obtained from the Arrhenius plots in Figure 6 with generally negative values for the gradient.

This means values of the activation energy E_a obtained were generally positive as listed in Table 2. To obtain the standard activation entropies (ΔS^o) and enthalpies (ΔH^o) of the corrosion process, the Eyring transition-state equation was employed (Abdallah et al., 2013; Manimegalai and Manjula, 2015):

$$CR = \frac{RT}{N_A} \exp\left(\frac{\Delta S^o}{R}\right) \exp\left(-\frac{\Delta H^o}{RT}\right) \qquad (10)$$

Linearizing by dividing both sides by T and taking the
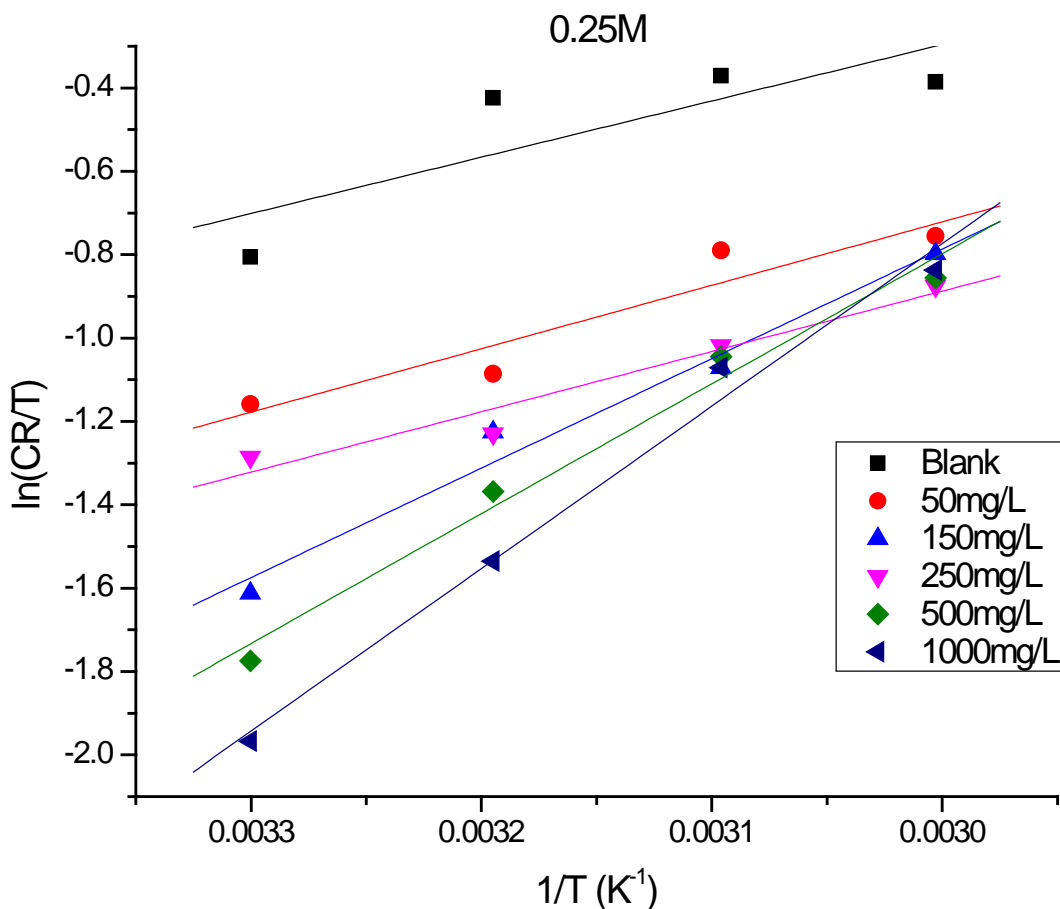
Figure 7. Transition State plot for Al alloy corrosion in 0.25 M HCl solution for blank and different concentrations of *Rosmarinus officinalis* L.

natural log of Equation 10 yields:

$$\ln\left(\frac{CR}{T}\right) = \left\{\ln\left(\frac{R}{N_A}\right) + \frac{\Delta S^o}{R}\right\} - \frac{\Delta H^o}{R}\left(\frac{1}{T}\right) \tag{11}$$

Figure 7 shows the plots of values of $\frac{1}{T}$ against $\ln\left(\frac{CR}{T}\right)$ from which values of ΔH^o and ΔS^o were computed from the gradient and intercept, respectively shown in Table 2.

According to Table 2, the calculated values of the activation energy E_a range from 15.29 kJ/mol to 35.06kJ/mol in the presence the *R. officinalis* L. leaves extract which are higher than the value of 13.87 kJ/mol

obtained in the blank solution suggesting a physisorption or the mix process f chemisphysisorption.

Moreover, values for E_a generally increased with increase in concentration of the *R. officinalis* L. leaves extract. This implies that the organic compounds such as flavonoids in rosemary leaves extract which act as passivating inhibitors inhibit Al alloy corrosion by increasing the energy barrier for charge and mass transfer. This is in agreement with the results reported in the literature by Abdallah et al. (2013) and Velázquez-González et al. (2014).

Calculated values of $\Delta H^o > 0$ were obtained and found to be higher in the presence of *R. officinalis L.* leaves extract than in its absence. This suggests that the Aluminium dissolution process is endothermic (Lyubchik et al., 2011) and agrees with results obtained by Abdallah et al. (2013) and Ating et al. (2010).

Al surface is associative rather than Small values of

Table 3. Some Adsorption isotherms and their parameters.

Model	Isotherm	Linear form	Equation	Reference
Langmuir	$kC = \dfrac{\theta}{1-\theta}$	$\ln\left(\dfrac{C}{\theta}\right) = \ln C - \ln k$	(12)	Beda et al, 2017
Villamil	$\dfrac{C}{\theta} = \dfrac{n_w}{k} + n_w C$	$\dfrac{C}{\theta} = \dfrac{n_w}{k} + n_w C$	(13)	Villamil et al., 1999
Freundlich	$\theta = kC^{y_n}$	$\ln\theta = \ln k + \dfrac{1}{n}\ln C$	(14)	Quinlan 2015
Temkin	$kC = \exp(-f\theta)$	$\theta = -\dfrac{\ln C}{f} - \dfrac{\ln k}{f}$	(15)	Bastidas et al., 2005
El-Awady	$(kC)^y = \dfrac{\theta}{1-\theta}$	$\ln\left(\dfrac{\theta}{1-\theta}\right) = \ln k' + y\ln C$	(16)	Beda et al, 2017
Dubinin-Radushkevich	$\ln\theta = \ln\theta_{\max} - \alpha\partial^2$	$\ln\theta = \ln\theta_{\max} - \alpha\delta^2$	(17)	Beda et al, 2017

Θ=Surface coverage=$I.E$/100; k=the adsorption equilibrium constant; C=concentration of the inhibitor; n_w=number of displaced water molecules from the adsorbent surface; 1/n=the adsorption intensity; f= molecular interaction parameter; y=number of inhibitor molecules occupying a given site; $k' = k^y$; Θ_{max}=maximum surface coverage.

$\Delta S^o < 0$ indicate a decrease in entropy at the transition state, that is, where the reactants from their initial state to the activation complex. With only a single activated complex exists in the slowest step of the reaction, that is, the rate determining step, this means the interaction between molecules of the inhibitor and that of the absorbent dissociative owing to the decrease in disorder. This result is similar to that reported by Abdallah et al. (2013).

Adsorption isotherms

Adsorption isotherms are simply graphs used for studying the nature and mechanism behind an adsorption process. The amount of adsorbate (*R. officinalis* L.) on the adsorbent is expressed as function of its pressure or concentration at constant temperature (Wilson et al., 1968). When molecules of the *R. officinalis* L. and the adsorbent Al metal are in contact long enough, an equilibrium is established between the adsorbed molecules on the adsorbent Al surface and the unadsorbed molecules of *R. officinalis* L. still left in the solution. This is the equilibrium relationship described by these isotherms (Lyubchik et al., 2011).

The adsorption isotherm models are generally of the form (Abdallah et al., 2013):

$$kC = g(\theta, \chi)\exp(-f\theta) \qquad (18)$$

where $g(\theta, \chi)$ is the configurational term parameter that characterizes the given isotherm model and its assumption(s) (Beda et al, 2017; Manimegalai and Manjula, 2015). The experimental data was fitted to the empirical models of the Lagmuir, Villamil, Freundlich, Temkin, and the kinetic-thermodynamic model of El-Awady. The equation for these models and all other parameters are defined in Table 3.

The Langmuir isotherm

According to literature by (Foo and Hameed, 2010) the Langmuir isotherm model characterizes a monolayer adsorption of the adsorbate molecules unto a fixed number of sites on the adsorbent metal surface. The adsorbate molecules are considered to be homogeneous, with all active sites possessing equal affinities for the adsorbate. Using the linearized form of the Langmuir isotherm model given in Equation 13, values of $\ln\left(\dfrac{C}{\theta}\right)$ plotted against $\ln C$ is shown in Figure 8. The values for $\ln k$ at different temperatures are obtained from the intercept of the graph. The changes in Gibb's free energy ΔG^o_{ads} for the adsorption of a molecule of the *R. officinalis* L. leaves extract unto the surface of the Al metal was calculated at various temperatures (in kJ/mol) and listed in Table 4 using the equation (Beda et al., 2017):

$$\Delta G^o_{ads} = -RT\ln(55.5k) \qquad (13)$$
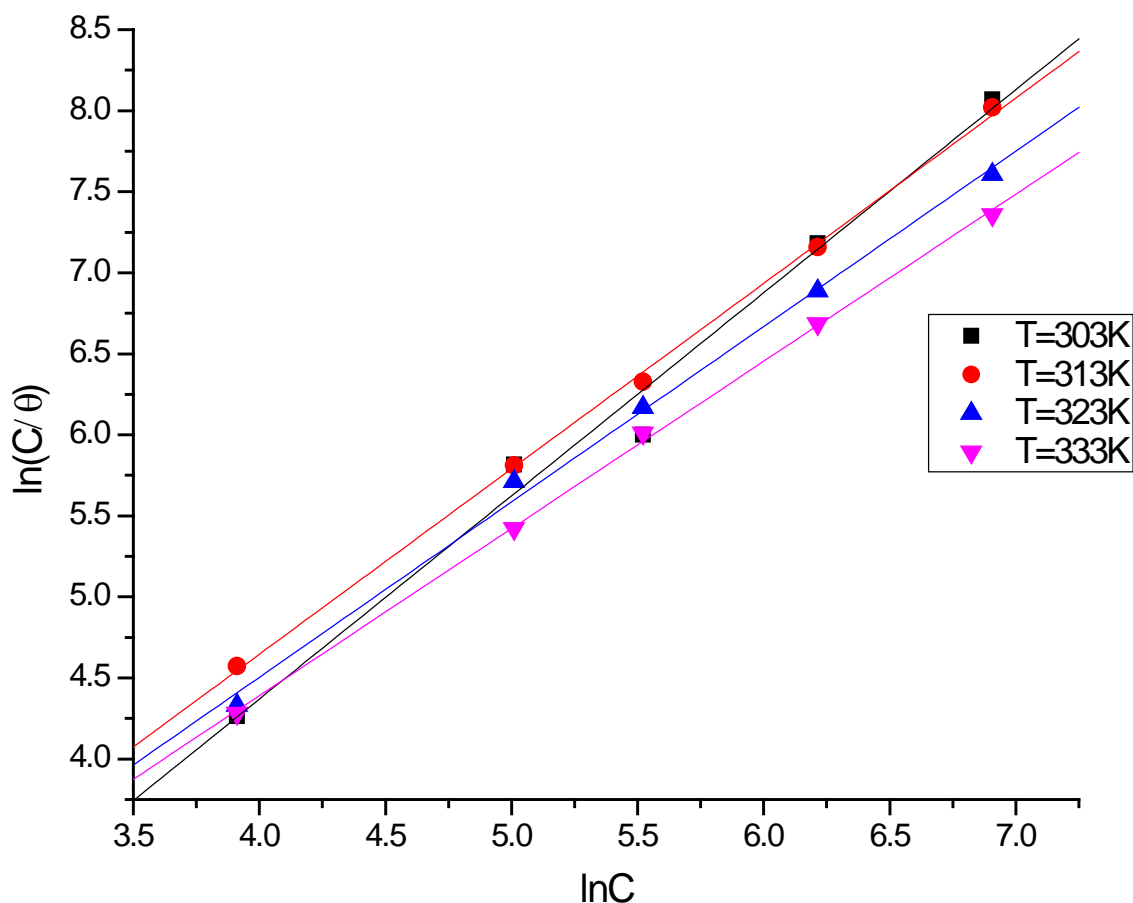
Figure 8. Langmuir adsorption isotherm plot for Al alloy corrosion in 0.25 M HCl solution for *Rosmarinus officinalis* L. extract at different temperatures.

Table 4. Parameters of linear regression from the Langmuir Isotherm plot for Al alloy corrosion in 0.25 M HCl solution for *Rosmarinus officinalis* L. extract at different temperatures.

Temperature (K)	ΔG°_{ads} (kJ/mol)	Slope	k	R^2
303	11.74	1.25343	1.9034	0.982
313	10.27	1.14398	0.9318	0.999
323	10.31	1.08194	0.8381	0.995
333	10.38	1.0313	0.7665	0.999

where the value 55.5 is the concentration of water in the solution in mol/L.

Values of the correlation coefficient was in the range $0.98 < R^2 < 0.99$ as shown in Table 4 suggesting that the corrosion data for 0.25 M HCl was a good fit for the Langmuir isotherm model. A similar result was reported by (Deyab, 2016) using ethanolic extract of rosemary on Al in biodiesel, and (Zhao et al, 2017) and (Chaubey et al, 2018) using triazinedithiol inhibitors for Al in 1.0 M HCl

and papaya peel extract on Al in 1.0 M HCl solution, respectively.

From Table 4, values of the slopes obtained were very close to unity suggesting that the molecules of *R. officinalis* L. form a monolayer on the Al alloy surface which is in agreement with the Langmuir model theory. Values of the equilibrium constant ($_k$) were also observe to decrease with increase in temperature. This implies that the inhibitor efficiency decreases with temperature.
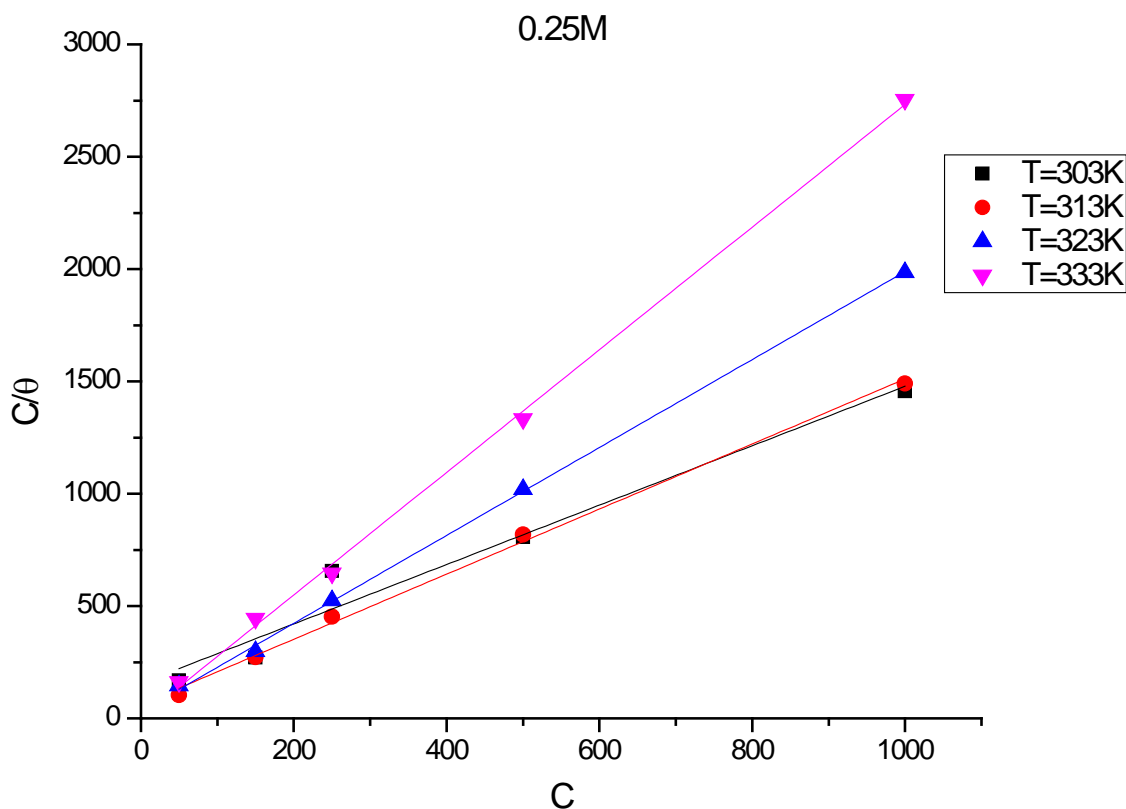
Figure 9. Villamil adsorption isotherm plot for Al alloy corrosion in 0.25 M HCl solution for *Rosmarinus officinalis* L. extract at different temperatures.

Calculated values of the Gibb's free energy (ΔG^o_{ads}) were negative, thereby signifying a spontaneous adsorption process (Ramachandran et al., 2011). Values for ΔG^o_{ads} ranged from -10.38 to -11.74 kJ/mol. This is indicative of physisorption. According to literature reported by (Ituen et al., 2017; Stango and Vijayalakshmi, 2018) values of $\left|\Delta G^o_{ads}\right| \le 20\text{kJ/mol}$ have typically been attributed to a weak Van der Waals or electrostatic forces of interaction between the molecules of the *R. officinalis* L. extract and active sites on the Al alloy surface.

The Villamil isotherm

This Villamil isotherm is a hybrid of the Langmiur isotherm model. It helps account for the shortcomings of the Langmuir model in that some isothermal slopes may deviate markedly from unity (Ituen et al, 2017) thereby indicative of a multilayer adsorption. Using the (Villamil et al., 1999) isotherm of Eqn (14), values of $\dfrac{C}{\theta}$ plotted against C are shown in Figure 9 below.

On observation of the plot in Figure 9, it was observed that the corrosion data for 0.25 M is a good fit for the Villamil model. This is supported by coefficient of correlation of correlation values ($R^2 > 0.95$) listed in Table 5.

According to literature reported by (Beda et al., 2017), the number of displaced water molecules from the adsorbent surface (n_w) is the constant introduced to account for the limitations of the Langmuir model. Values of n_w obtained from the slopes of the isotherms in Figure 10 were observed to increase with increase in temperature. This suggests that a multilayer adsorption predominates at elevated temperatures. The values for the equilibrium constant (k) obtained from the intercepts of the isotherms were observed to increase with increase in temperature. This could mean that the inhibitor efficiency increased with increase in temperature for the 0.25 M HCl solution.

The Freundlich, Temkin and El-Awady isotherms

It is clear from Table 5 that empirical models like the

Table 5. Parameters of linear regression from the Villamil Isotherm plot for Al alloy corrosion in 0.25 M HCl solution for *Rosmarinus officinalis* L. extract at different temperatures.

Temperature (K)	ΔG°_{ads} (kJ/mol)	n_w	intercept	k	R^2
303	1.90	1.3220	155.9432	0.0085	0.950
313	-0.65	1.4484	62.5129	0.0232	0.997
323	-3.32	1.9570	31.5797	0.0620	0.999
333	-10.56	2.7293	3.3467	0.8155	0.999
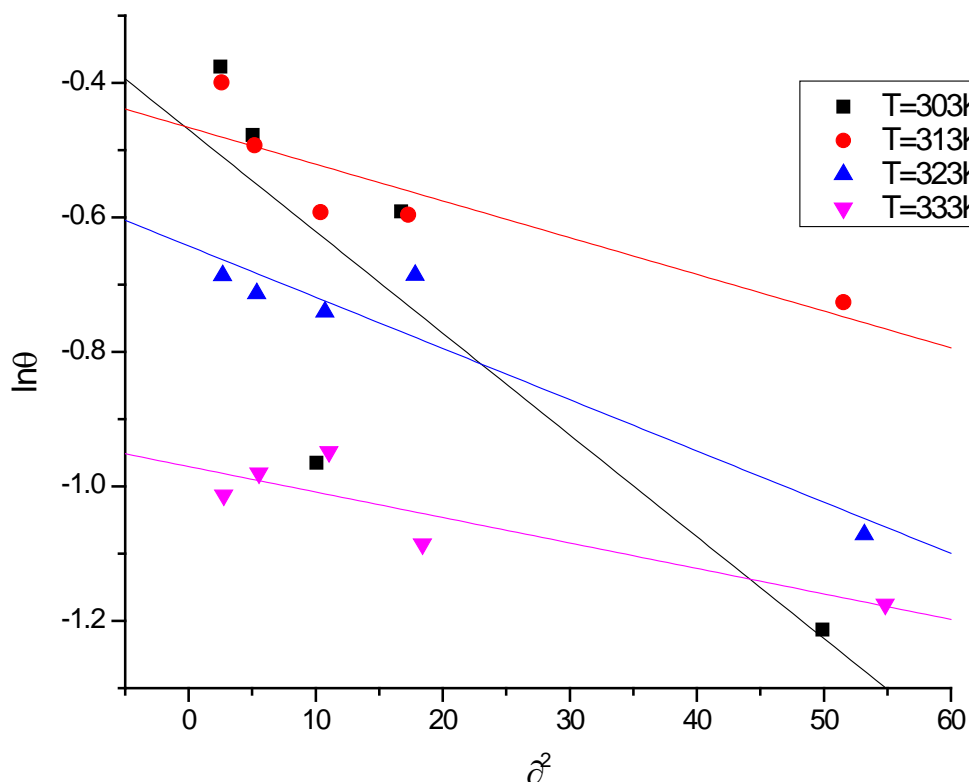
Figure 10. Dubinin-Radushkevich adsorption isotherm plot for Al alloy corrosion in 0.25 M HCl solution for *Rosmarinus officinalis* L. extract at different temperatures.

Freundlich and Temkin and the kinetic-thermodynamic isotherm of the El-Awady were not really a good fit for the experimental data with values of the correlation coefficient in the range ($0.16 < R^2 < 0.98$) for the Freundlich isotherm, ($0.42 < R^2 < 0.95$) for Temkin, and ($0.44 < R^2 < 0.94$) for the isotherm of El-Awady.

Based on the results summarized in Table 6, the conclusion that values of the Gibb's free energy (ΔG°_{ads}) obtained at elevated temperatures were low and more negative than the values at room temperature can be arrived at. This suggests that an increase in temperature increases the spontaneity of the adsorption process. A similar result was reported by Ating et al. (2010) using the ethanolic extract of *Ananas sativum* for Al in 0.1 M HCl solution. Values for the adsorption intensity ($\frac{1}{n}$) obtained from the Freundlich model were very close to zero. This means the adsorption process was favourable, relatively easy, and suggests that the adsorbent Al alloy surface becomes more heterogeneous with increase in temperature (Quinlan, 2015). Moreover, negative values for the interaction parameter (f) suggest lateral repulsion taking place in the adsorbed layer (Bastidas et al., 2005). From the kinetic-thermodynamic model of El-Awady shows that values of y decreased with increase in temperature which means the number of *R. officinalis*

Table 6. Calculated values of the Adsorption and Linear regression parameters of isotherm plots for the adsorption of *Rosmarinus offinalis* L. on to Al alloy.

Isotherm	Temperature (K)	ΔG°_{ads} (kJ/mol)	1/n	$\ln k$	k	R^2
Freundlich	303	-4.6634	0.26131	-2.1652	0.1147	0.630
	313	-7.4753	0.10565	-1.1438	0.3186	0.964
	323	-7.0093	0.11371	-1.4063	0.2451	0.499
	333	-7.3104	0.06081	-1.3759	0.2526	0.451

Isotherm	Temperature (K)	ΔG°_{ads} (kJ/mol)	Slope	f	k	R^2
Temkin	303	-6.71	0.1221	-8.2	0.2580	0.641
	313	-20.88	0.06028	-16.6	55.0072	0.950
	323	-22.33	0.04722	-21.2	73.6592	0.499
	333	-43.39	0.02064	-48.5	115494.3332	0.421

Isotherm	Temperature (K)	ΔG°_{ads} (kJ/mol)	y	1/y	k'	R^2
El-Awady	303	-3.04	0.5147	1.9	0.2356	0.657
	313	-7.66	0.2496	4.0	0.7649	0.943
	323	-7.48	0.1957	5.1	0.7861	0.499
	333	-8.05	0.0921	10.9	0.9028	0.435

L. molecules occupying an active site on the Al alloy surface decreased at elevated temperatures. Furthermore, values of $\dfrac{1}{y} > 1$ ranged from 2 to about 11, thus signifying that a given molecule of *R. officinalis* L. occupies more than one active site.

As depicted in Table 6, values of the adsorption constant (k') increased with increase in temperature indicating that the adsorption of the *R. officinalis* L. extract molecules unto the Al surface is favourable at elevated temperatures in the 0.25 M HCl solution.

The Dubinin-Radushkevich isotherm

In order to discriminate between physical and chemical adsorption (Beda et al., 2017; Foo and Hameed, 2010; Ayawei et al., 2017) at the adsorbate-adsorbent interface the Dubinin-Radushkevich isotherm model is used.

From Table 3, we recall Equation 18 for the model to be:

$$\ln \theta = \ln \theta_{\max} - \alpha \partial^2$$

where ∂ is the Polanyi potential (Beda et al., 2017 which is given by:

$$\partial = RT \ln \left(1 + \frac{1}{C}\right) \tag{14}$$

Furthermore, the isotherm constant (α) is related to the mean free energy per molecule of adsorbate, E_m as:

$$E_m = \frac{1}{\sqrt{2\alpha}} \tag{15}$$

Plotting values of $\ln \theta$ against ∂^2 at all temperatures for the 0.25 M HCl solutions as shown in Figure 10, values for the isotherm constant (α), and the maximum surface coverage ($\theta_{\max}$) can be obtained from the slopes and intercepts of the isotherms, respectively.

The experimental data for 0.25 M HCl was moderately good fit with values for the correlation coefficient in the range ($0.58 < R^2 < 0.87$) as listed in Table 7. Calculated values for the mean free energy per molecule (E_m) of the *R. officinalis* L. extract increased with increase in temperature. The maximum surface coverage decreased with increase in temperature implying that the adsorption process was less favourable at elevated temperatures. Furthermore, values of E_m plotted against T help discriminate between physical and chemical adsorption; according to the literature reported by (Beda et al., 2017), values of E_m less than and greater than 8 kJ/mol suggest physisorption and chemisorption, respectively.

Figure 11 shows that physisorption predominates at T=303K, while the adsorption of molecules of the inhibitor

Table 7. Parameters of linear regression from the Dubinin-Radushkevich isotherm plot for Al alloy corrosion in 0.25 M HCl solution for *Rosmarinus officinalis* L. extract at different temperatures.

Temperature (K)	α (kJ^{-2} mol^2)	intercept	θ_{max}	E_m (kJ/mol)	R^2
303	0.0151	-0.4697	0.6252	5.75	0.578
313	0.0055	-0.4663	0.6273	9.53	0.711
323	0.0076	-0.6425	0.5260	8.11	0.867
333	0.0038	-0.9705	0.3789	11.47	0.704
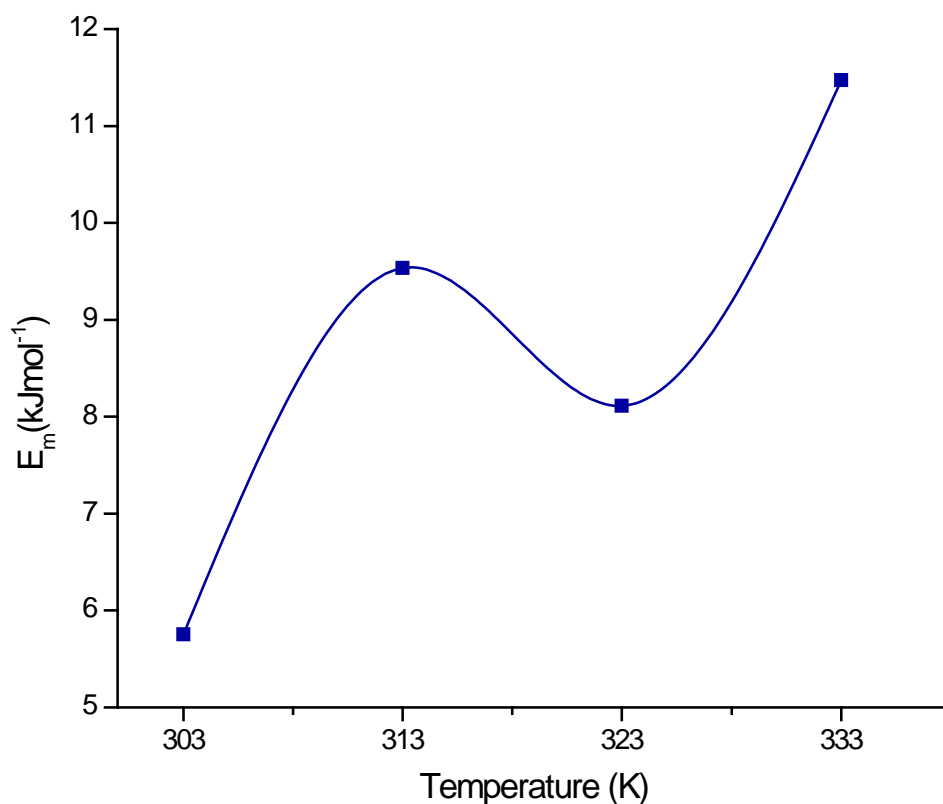
Figure 11. Mean adsorption energy against temperature for Al alloy corrosion in 0.25 M HCl solution using *Rosmarinus officinalis* L. extract.

unto the adsorbent Al alloy surface solution takes a more chemical nature as the temperature approaches 313K and above. A similar result was reported in the literature by (Beda et al., 2017).

From Table 7, values of θ_{max} generally decrease with increase in temperature. This confirms a decrease in the rate of adsorption with increasing temperature.

Effect of an external magnetic field

The aim of this experiment was to study the effects of an externally applied magnetic field on the corrosion Al alloy AA8011 by HCl both in the presence and absence of the *R. officinalis* L. extract.

The corrosion data obtained under the influence of a magnetic field (B) in the 0.25 M HCl solution for the blank and inhibited experiments at 303K are listed in Table 8.

Figure 12 shows that the results obtained in at lower concentrations of the *R. officinalis* L. extract below 250 mg/L reveal that the corrosion rate of Al increases in the presence of a magnetic field than in the absence of it. It appears that the presence of a magnetic field enhances the dissolution of Al in the 0.25 M HCl solution.

Table 8. Values of the corrosion rate at room temperature both in the absence and absence of a magnetic field in 0.25M HCl solution for blank and at various concentration of the inhibitor.

Concentration (mg/L)	Corrosion rate (mm/year)			
	B=0	B≠0		
	V=0.0 V	V=15.0 V	V=20.0 V	V=25.0 V
Blank	135.33	139.40	144.92	173.95
50	95.09	139.26	108.91	105.25
150	60.41	103.15	89.37	88.87
250	83.77	67.03	69.83	72.51
500	51.40	49.90	47.88	46.24
1000	42.38	40.77	37.93	37.96
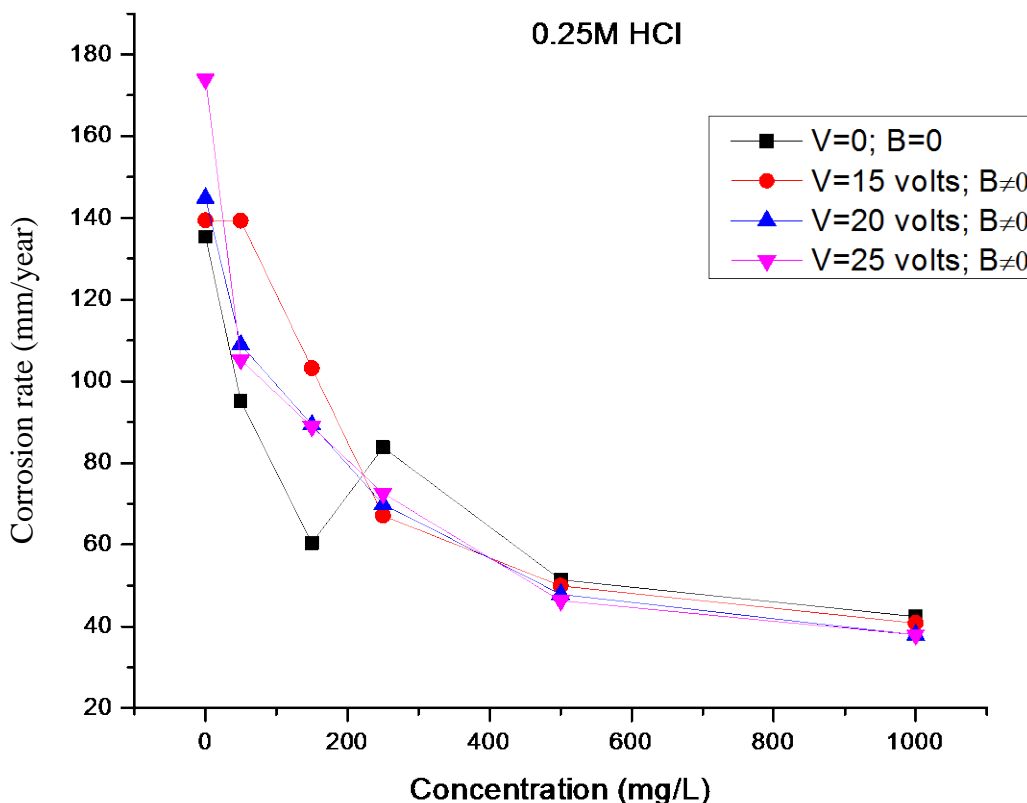
Figure 12. Plot of corrosion rate against concentration for Al alloy at room temperature both in the absence and absence of a magnetic field in 0.25 M HCl solution.

A similar result was reported in the literature by (Rousan and Al-Rawashdeh, 2006). However, above the 250 mg/L limit, the corrosion rate is suppressed in the presence of the magnetic field with increasing concentrations of the *R. officinalis* L. extract, this could mean that the presence of the magnetic field and an increase in the concentration of the inhibitor above 250 mg/L enhanced the passivation of Al. At concentrations of the inhibitor it was observed that an increase in the strength of the magnetic field (with increase in voltage) also suppresses the corrosion rate of Al.

Conclusion

R. officinalis L. leaf extract was found to be a viable corrosion inhibitor for aluminium alloy AA801 in aqueous solution of 0.25 M HCl. The inhibition efficiency decreased

with temperature but increased with concentration of the extract up to 1000 mg/L. The adsorption of the rosemary extract obeys the adsorption isotherm models of Langmuir and the Villamil. The negative values of the adsorption free energy (ΔG_{ads}°) and positive values of the adsorption enthalpy (ΔH_{ads}°) suggest a spontaneous and endothermic process. Values for the activation energy (E_a) indicated the presence of physisorption and chemisorption, this result was in agreement with results obtained from the Dubinin-Radushkevich isotherm model. The effect of an external magnetic field was found to generally suppress the corrosion rate of the Al alloy at room temperature only for concentrations of the extract above 250 mg/L. Moreover, the corrosion rate was found to decrease with increase in strength of the magnetic field.

CONFLICT OF INTERESTS

The authors have not declared any conflict of interests.

REFERENCES

Abdallah M, Zaafarany I, Fawzy A, Radwan MA, Abdfattah E (2013). Inhibition of Aluminum Corrosion in Hydrochloric Acid by n-, Di-n- and Tri-n-Butylamines. Corrosion 22(3):53-59 doi: 10.5006/0010-9312-22.3.53.

Ating EI, Umoren SA, Udousoro II, Ebenso EE, Udoh AP (2010). Leaves extract of *ananas sativum* as green corrosion inhibitor for aluminium in hydrochloric acid solutions. Green Chemistry Letters and Reviews 3(2):61-68. doi: 10.1080/17518250903505253.

Ayawei N, Ebelegi AN, Wankasi D (2017). Modelling and Interpretation of Adsorption Isotherms. Journal of Chemistry. doi: 10.1155/2017/3039817.

Barbut S, Josephson DB, Maurer AJ (1985). Antioxidant Properties of Rosemary Oleoresin in Turkey Sausage. Journal of Food Science 50(5):1356–1359 doi: 10.1111/j.1365-2621.1985.tb10476.x.

Bastidas DM, Gómez PP, Cano E (2005). The isotherm slope. A criterion for studying the adsorption mechanism of benzotriazole on copper in sulphuric acid. Review Metal 41(2):98-106 doi: 10.3989/revmetalm.2005.v41.i2.192.

Beda RHB, Niamien PM, Avo Bilé EB, Trokourey A (2017). Inhibition of Aluminium Corrosion in 1.0 M HCl by Caffeine: Experimental and DFT Studies. Advances in Chemistry, pp. 1-10, doi: 10.1155/2017/6975248.

Catic S, Obralic E, Bratoviv A (2016). Rosemary as ecologically acceptable corrosion inhibitor of steel pp. 3-6.

Chaubey N, Singh VK, Quraishi MA (2018). Papaya peel extract as potential corrosion inhibitor for Aluminium alloy in 1 M HCl: Electrochemical and quantum chemical study. Ain Shams Engineering Journal 9(4):1131-1140 doi: 10.1016/j.asej.2016.04.010.

Davis JR (1993). Aluminum and Aluminum Alloys - Google Books. In: Aluminum and Aluminum Alloys, pp. 13–17.

Deya MA (2016). Corrosion inhibition of aluminum in biodiesel by ethanol extracts of Rosemary leaves. Journal of the Taiwan Institute of Chemical Engineers 58:536-541. doi: 10.1016/j.jtice.2015.06.021.

El Maghraby AA (2009). Corrosion Inhibition of Aluminum in Hydrochloric Acid Solution Using Potassium Iodate Inhibitor. The Open Corrosion Journal 2(1):189-196 doi: 10.2174/1876503300902010189.

El-Awady AA, Abd-El-Nabey BA, Aziz SG (1993). Thermodynamic and kinetic factors in chloride ion pitting and nitrogen donor ligand inhibition of aluminium metal corrosion in aggressive acid media. Journal of the Chemical Society, Faraday Transactions 89(5):795-802 doi: 10.1039/FT9938900795.

Foo KY, Hameed BH (2010). Insights into the modeling of adsorption isotherm systems. Chemical Engineering Journal 156(1):2-10 doi: 10.1016/j.cej.2009.09.013.

Fouda AS, Nofal AM, El-Ewady GY, Abousalem AS (2015). Eco-friendly impact of rosmarinus officinalis as corrosion inhibitor for carbon steel in hydrochloric acid solutions. Der Pharma Chemcia 7(5):183-197.

Francis NO, Owate IO, Osarolube E (2019). Electrochemical Corrosion Inhibition Process, Adsorption Mechanism and Mechanical Effect of Newbouldia laevis Leaf Extract on Aluminum Alloy in Acidic Environment. Physical Science International Journal. 20(4):1-12, doi: 10.9734/psij/2018/46346.

Gilbert PT (1978). What is corrosion? British Corrosion Journal 13(4):153-153. doi: 10.1179/000705978798276131.

Hansson CM (2011). The impact of corrosion on society. Metall. Mater. Trans. A Physics of Metals and Metallography Science 42(10):2952-2962. doi: 10.1007/s11661-011-0703-2.

Ibisi NE, Uwakwue VI (2015). Cnestis ferruginea as eco-friendly corrosion inhibitor of mild steel in corrosive environment. Global Journal of Environmental Science and Technology 2(6):355-359,.

Ituen E, Akaranta O, James A (2017). Evaluation of Performance of Corrosion Inhibitors Using Adsorption Isotherm Models: An Overview. Chemical Science International Journal 18(1):1-34 doi: 10.9734/csji/2017/28976.

Jegdić B, Popić, J, Bobić B, Stevanović M (2016). Chemical corrosion of metals and alloys. Zast. Mater 57(2):205-211. doi: 10.5937/zasmat1602205j.

Kesavan D, Gopiraman M, Sulochana N (2012). Green Inhibitors for Corrosion of Metals : A Review Correspondence. Chemical Science Review and Letters 1(1):1-8.

Khan G, Newaz KMS, Basirun WJ, Ali HBM, Faraj FL, Khan GM (2015). Application of natural product extracts as green corrosion inhibitors for metals and alloys in acid pickling processes- A review. International Journal of Electrochemical Science 10(8):6120–6134.

Lowson RT (1978). Aluminium Corrosion Studies. IV: Pitting Corrosion. Australian Journal of Chemistry 31(5):943-956. doi: 10.1071/CH9780943.

Lyubchik S, Lyubchik A, Lygina O, Lyubchik S, Fonsec I (2011). Comparison of the Thermodynamic Parameters Estimation for the Adsorption Process of the Metals from Liquid Phase on Activated Carbons. Thermodyn. - Interact. Stud. - Solids, Liq. Gases, pp. 4-122, doi: 10.5772/19514.

Manimegalai S, Manjula P (2015). Thermodynamic and adsorption studies for corrosion inhibition of mild steel in aqueous media by Sargasam swartzii (Brown algae). Journal of Materials and Environmental Science 6(6):1629-1637,.

Millberg LS (2018). How aluminum foil is made - material, manufacture, making, used, processing, dimensions, aluminium, procedure. Madehow.Com, 2018. [Online]. Available: http://www.madehow.com/Volume-1/Aluminum-Foil.html. [Accessed: 08-Mar-2020].

Myers HP (1997). Introductory Solid State Physics. In Introductory Solid State Physics. https://doi.org/10.4324/9780203212554

Nakatani N (2000). Phenolic antioxidants from herbs and spices. BioFactors 13(1-4):141-146, doi: 10.1002/biof.5520130123.

Noor EA (2009). Potential of aqueous extract of Hibiscus sabdariffa leaves for inhibiting the corrosion of aluminum in alkaline solutions. Journal of Applied Electrochemistry 39(9):1465-1475. doi: 10.1007/s10800-009-9826-1.

Nwosu FO, Owate IO, Osarolube E (2018). Acidic Corrosion Inhibition Mechanism of Aluminum Alloy Using Green Inhibitors 8(3):45-50, doi: 10.5923/j.materials.20180803.01.

Patni N, Agarwal S, Shah P (2013). Greener Approach towards Corrosion Inhibition. Chinese Journal of Engineering pp. 1-10, doi: 10.1155/2013/784186.

Philip PE, Schweitzer A (2003). Metallic Materials Physics, Mechanical

and Corrosion Properties. PROVIDE SOURCE/LINK

Popoola API, Fayomi OSI, Abdulwahab M (2012). Degradation behaviour of aluminium in 2M HCl/HNO 3 in the presence of Arachis hypogeae natural oil. International Journal of Electrochemical Science 7(7):5817-5827.

Quinlan PJ (2015). The design and optimization of sustainable biopolymer-based adsorbents for the removal of a model aromatic naphthenic acid from aqueous solution. (Master's thesis, University of Waterloo).

Ramachandran P, Vairamuthu R, Ponnusamy S (2011). Adsorption isotherms, kinetics, thermodynamics and desorption studies of reactive orange16 on activated carbon derived from *ananas comosus* (L.) carbon. Journal of Engineering and Applied Sciences 6(11):15-26.

Rani BEA, Basu BBJ (2012). Green inhibitors for corrosion protection of metals and alloys: An overview. International Journal of Corrosion 2012 doi: 10.1155/2012/380217.

Rousan AA, Al-Rawashdeh NAF (2006). Magnetic field effects on inhibition of aluminium corrosion by cationic surfactant in acidic solution. Corrosion Engineering, Science and Technology 41(3):235-239, doi: 10.1179/174327806X132150.

Saha P, Chowdhury S (2011). Insight into adsorption thermodynamics. Thermodynamics 16:349-364.

Sangeetha M, Rajendran S, Sathiyabama J, Krishnaveni A (2013). Inhibition of corrosion of aluminium and its alloys by extracts of green inhibitors. Portugaliae Electrochimica Acta 31(1):41-52 doi: 10.4152/pea.201301041.

Stango XSA, Vijayalakshmi U (2018). Studies on corrosion inhibitory effect and adsorption behavior of waste materials on mild steel in acidic medium. Journal of Asian Ceramic Societies 6(1):20-29 doi: 10.1080/21870764.2018.1439608.

Sukiman NL, Zhou X, Birbilis N, Hughes AE, Mol JM, Garcia SJ, Zhou X, Thompson GE (2012). Durability and corrosion of aluminium and its alloys: overview, property space, techniques and developments. Aluminium Alloys-New Trends in Fabrication and Applications 5:47-97.doi: 10.5772/3354.

Velázquez-González MA, Gonzalez-Rodriguez JG, Valladares-Cisneros MG, Hermoso-Diaz IA (2014). Use of <i>Rosmarinus officinalis</i> as Green Corrosion Inhibitor for Carbon Steel in Acid Medium. American Journal of Analytical Chemistry 5(2):55-64, doi: 10.4236/ajac.2014.52009.

Villamil RFV, Corio P, Agostinho SML, Rubim JC (1999). Effect of sodium dodecylsulfate on copper corrosion in sulfuric acid media in the absence and presence of benzotriazole. Journal of Electroanalytical Chemistry 472(2):112-119, doi: 10.1016/S0022-0728(99)00267-3.

Wilson JM, Newcombe RJ, Denaro AR, Rickette RMW (1968). Adsorption Isotherm. Experiments in Physical Chemistry pp. 85-87.

Zhao Q, Tang T, Dang P, Zhang Z, Wang F (2017). The corrosion inhibition effect of triazinedithiol inhibitors for aluminum alloy in a 1 M HCl solution. Metals (Basel) 7(2):1-11 doi: 10.3390/met7020044.